The Magdalena Ridge Observatory Interferometer: Custom Near-IR Beamsplitter and AR Coatings

[a] E.K. Block, [a] C.A. Jurgenson [b] D.F. Busher, [b] C.A. Haniff, , [b] J.S. Young, [a] M.J.Creech-Eakman, [c] A. Jaramillo, [c] R. Schnell

[a] New Mexico Institute of Mining and Technology, 801 Leroy Place, Socorro, NM 87801 ,USA;
[b] Cavendish Laboratory, J. J. Thomson Avenue, Cambridge CB3 0HE, U.K.;
[c] Optical Surface Technologies, 2801 Unit E Broadbent Parkway N.E., Albuquerque, NM 87107

ABSTRACT

This report focuses on the design, application, and testing of custom beamsplitter and anti-reflection coatings for use in the Magdalena Ridge Observatory Interferometer (MROI) beam combiners. The fringe tracker and science combiners will operate across the J, H, and K bands. The coatings were designed to achieve three optical characteristics critical to optical interferometry: 1) minimized stress of the substrate (leading to induced wavefront errors), 2) high throughput, and 3) high visibilities in broadband unpolarized light. The AR coating has less than 1% reflection losses. Beamsplitter coatings experienced visibility losses less than 1% due to group delay dispersion and s and p phase differences.
.

INTRODUCTION & BACKGROUND

The Magdalena Ridge Observatory is building an optical/infrared (0.6-2.4 micron) imaging interferometer. The main science goal is to deliver model independent images of faint and complex astronomical targets with milli-arcsecond spatial resolutions. The array will comprise10x1.4-meter telescopes arranged in an equilateral "Y" configuration **(Fig 1).** The infrastructure will support 28 foundation pads, allowing for 4 array configurations of the 10 telescopes with baseline of 7.5 to 340 m. Three custom coating have been designed for the near-infrared fringe tracking instrument that will support the ambitious top level science goals.

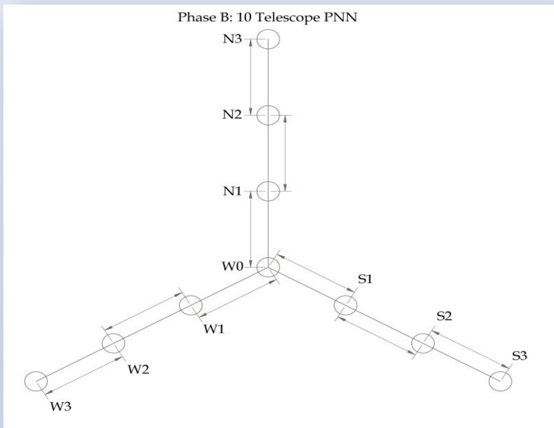

Fig 1 –2D schematic showing the hypothetical telescope array layout with nearest neighbor pair combinations (designated by the arrows). Individual telescopes are labeled by position: north (N), south (S), and west (W). A dedicated fringe tracker is being built to phase up the array through baseline bootstrapping. (Armstrong, J.T., Mozurkewich, D.,Pauls, T.A., Haiian, A.R., *Bootstrapping the NPOI: keeping long baselines in phase by tracking fringes on short baselines*, SPIE Vol. 3350, p. 461-466)

THE FRINGE TRACKER BEAM COMBINER

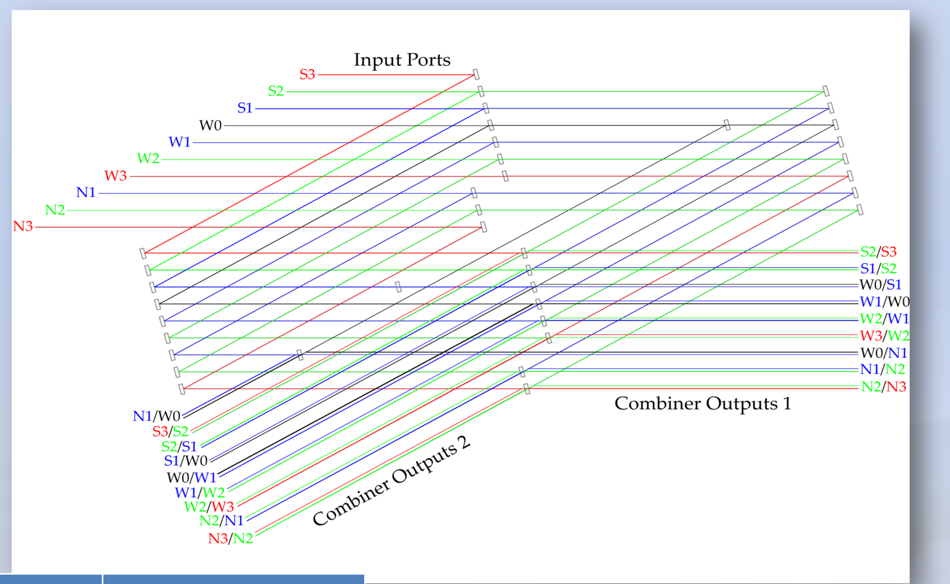

Path Pair Combinations	Number of Occurrences
A-B (e.g. S3/S2)	2
C-B (e.g. W1/W2)	3
D-E (e.g. S1/W0)	1
F-B (e.g. W0/W1)	1
C-G (e.g. W2/W3)	1
C-H (e.g. W0/N1)	1

Fig 2 -- 2D schematic of the FT beam combiner layout showing inputs and outputs from all 10 telescopes. Beams enter from the top left and exit at bottom right and left, in pairs that have interfered.

Table 1 – This table shows pair combinations and the number of times they occur.

The fringe tracker will operate in both the H (1.5-1.8 μm) and K_s (2.0-2.31 μm) bands. The FT layout (**Figure 2**) shows light from 10 unit telescopes (UTs) entering at the upper left and exiting at the two complementary combiner outputs: 1 (right reflected/left transmitted: RR/LT) and 2 (right transmitted/left reflected: RT/LR).

Because beams in the combiner traverse various components in different directions and in different orders, there exist unique paths (labeled A thru H) through the combiner that are not all identical in detail. These eight unique paths comprise six non-redundant combination pairs: A-B, C-B, D-E, F-B, C-G, C-H; **Figure 3** (below) shows their differences explicitly. Given the coating properties it is the differences between these paths that needs to be analyzed – in particular, how the coating properties and these differences impact the interferometric performance.

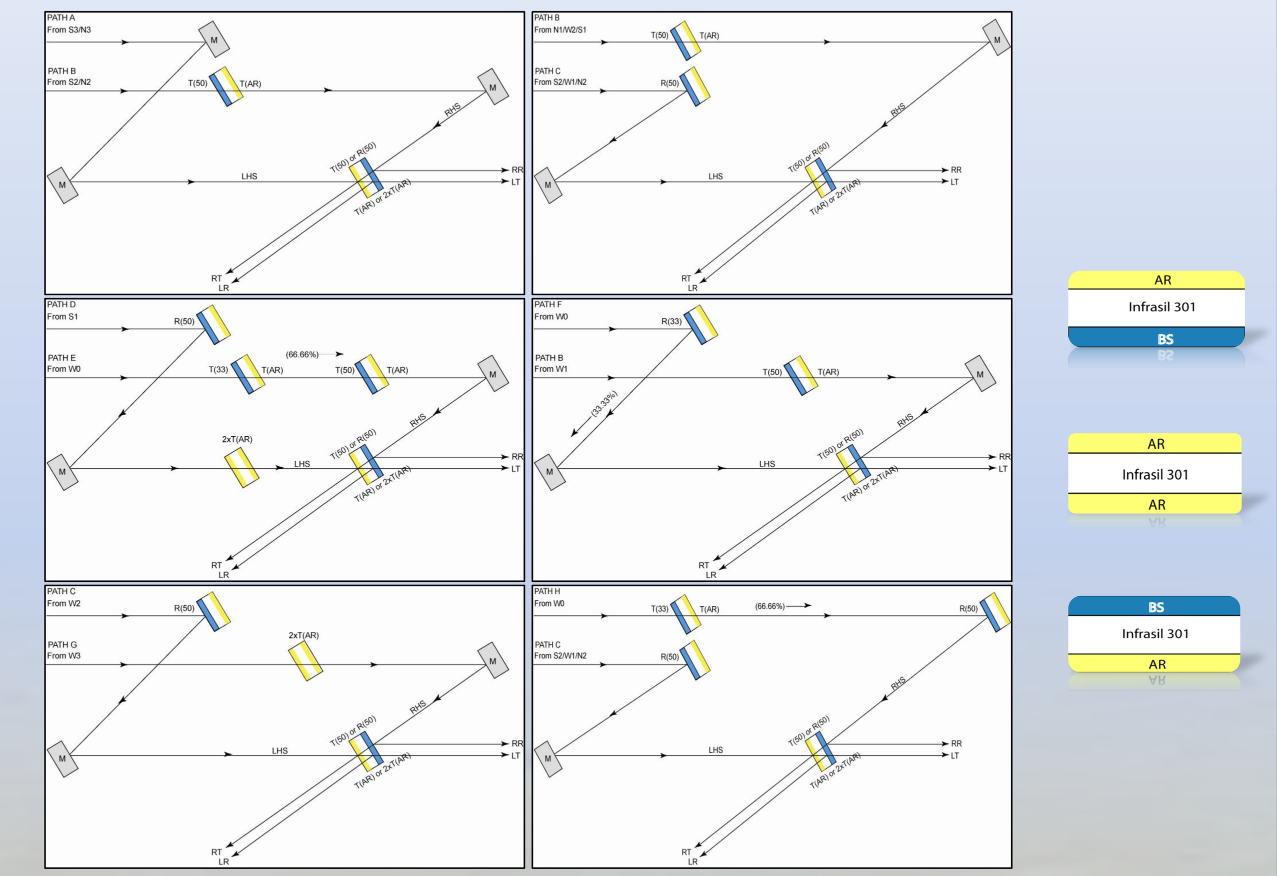

Fig 3 – 2D schematic of each combination pair. From left to right : A-B, C-B, D-E, F-B, C-G, C-H.

Abbreviations:
Gold coated mirrors (M),Transmission/Reflection 50% beamsplitter [T(50)/R(50)],Transmission/Reflection 33.33% beamsplitter [T(33)/R(33)], Transmission Anti-reflection [T(AR)], left hand side beam (LHS), right hand side beam (RHS), Right reflected (RR), Right transmitted (RT), Left Reflected (LR) , Left Transmitted (LT)

THEORETICAL COATING PERFORMANCE

Infrasil 301 was chosen as the substrate for all beamsplitter and compensator plates within the beam combiner. There are three different coatings which will be applied[1] to the Infrasil substrates[2]:

1. Anti-reflection (AR) coating
2. 33.33% reflectance beamsplitter coating
3. 50% reflectance beamsplitter coating

The AR coatings are applied to both sides of the compensator plates and one side of each beamsplitter plate. Only one plate receives the 33.33% reflective coating; the first beamsplitter encountered by the central telescope (W0 in **Figure 2**). The AR coating is optimized[3] for operation in the J, H, and K bands (1.1 μm to 2.4 μm) allowing it to be used by both the FT and IR science combiner. The beamsplitter coatings, only used in the FT, were optimized for operation in the H and K_s bands (1.5 μm to 2.31 μm).

All coatings consist of a top layer of MgF_2 followed by alternating layers of Nb_2O_5 and SiO_2. The AR coating is comprised of 14 layers with a total thickness of 1431.75 nm, the 33.33% beamsplitter coating is comprised of 9 layers with a total thickness of 1475.6 nm and the 50% beamsplitter coating is comprised of 8 layers with a total thickness of 1846.9 nm. **Figures 4-6** show the theoretical performance plots of the coatings in terms of the s, p polarization and mean reflectance as a function of wavelength. From these plots it can be seen that all coatings are very good with top level performance.

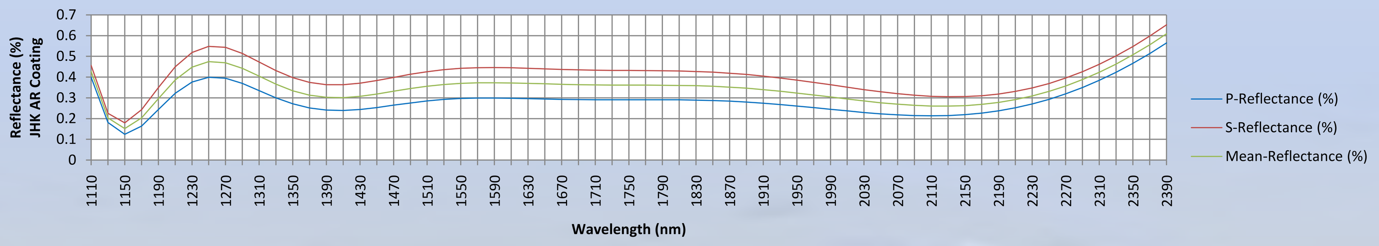

Fig 4 – The theoretical s, p and mean reflectance of the JHK AR coating as a function of wavelength.

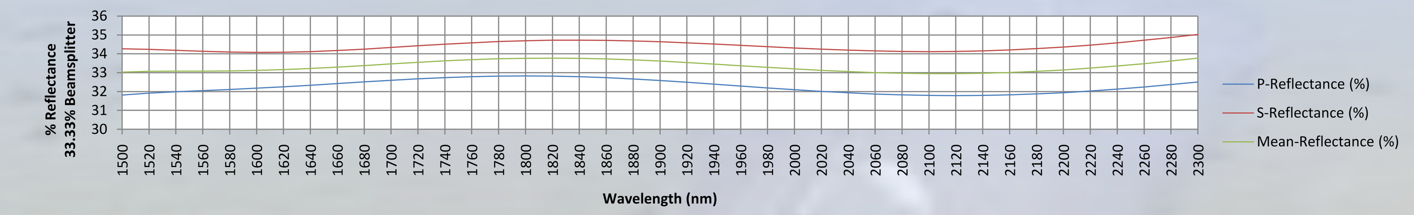

Fig 5 – The theoretical s, p, and mean reflectance of the 33.33% beamsplitter coating as a function of wavelength

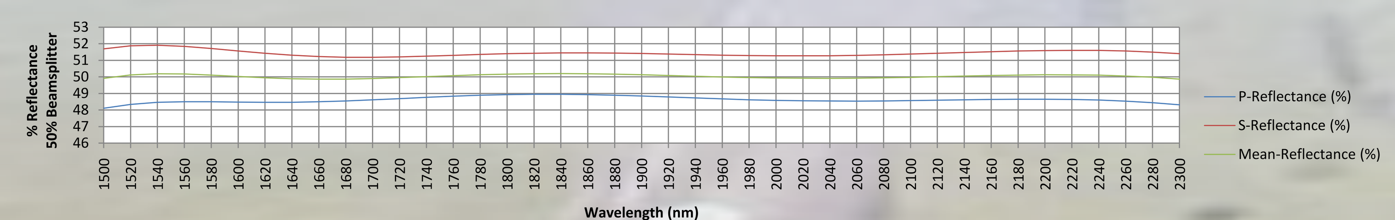

Fig 6 – The theoretical s, p, and mean reflectance of the 50% beamsplitter coating as a function of wavelength.

BEAM PATHS AT THE COMBINER PLATES

In all cases, pairs of beams in the fringe tracking combiner will interfere at a beam combiner plate. The trajectories of a typical pair of right- and left-ward propagating beams towards and through such a plate are shown in **Figure 7**. Note that the reflected LHS beam passes through the AR coating twice, while all other beams only traverse the coating once.

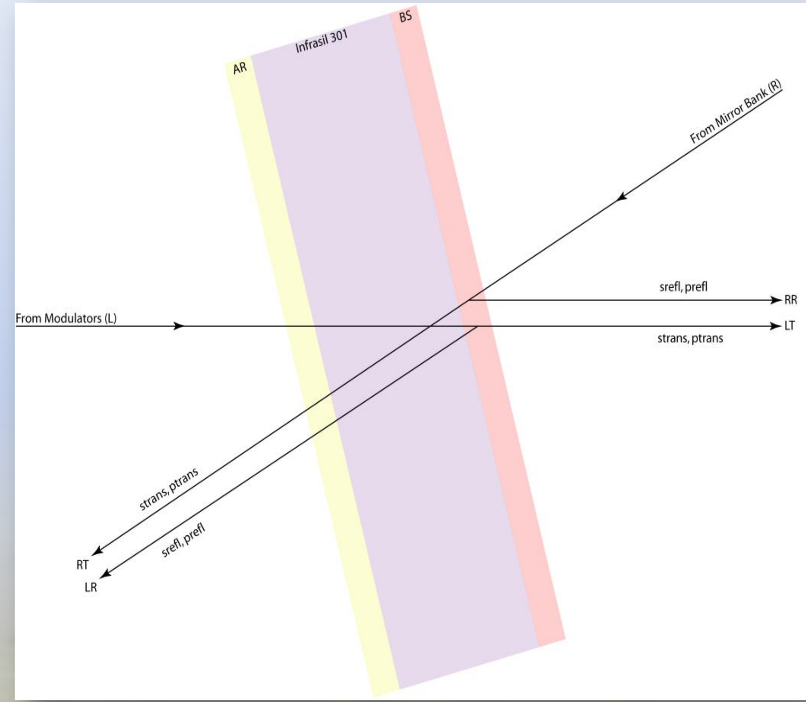

Fig 7 – A diagram representing the 50% beamsplitter combination point.

COMPUTING THE VISIBILITY LOSS FACTORS

For each unique combination path (see **Table 1**, **Figure 3**), visibility loss due to intensity mismatch ($V_{mismatch}$), s and p phase differences (V_{pol}), and the phase differences between combined wavefronts; group delay (V_{gd}) were calculated for all wavelengths in the H and K_s bands (1500-2300 nm) using equations **1**, **2** and **3**. Equation parameters are: $\rho = I_{refl}/I_{trans}$, $\varphi_{sp} = \varphi_p - \varphi_s$, $\Lambda_{coh} = Resolution*\lambda$, and $\delta_{gd} = \delta_{refl} - \delta_{trans}$.

$$V_{mismatch} = \frac{2}{\rho^{+1/2} + \rho^{-1/2}} \quad (1) \qquad V_{pol} = \left|\cos\left(\frac{\phi_{sp}}{2}\right)\right| \quad (2) \qquad V_{gd} = \frac{\sin\left[\pi \frac{\delta_{gd}}{\Lambda_{coh}}\right]}{\pi\left(\frac{\delta_{gd}}{\Lambda_{coh}}\right)} \quad (3)$$

CONCLUSIONS

- ✓ Coatings will not be the limiting factor in the performance of the FT beam combiner.
- ✓ Coatings meet the top level science goals for the MROI.
- ✓Greatest visibility losses arise from intensity mismatch. Losses due to polarization and group delay are small (<1 %).
- ✓ Overall theoretical visibility losses are ≤ 6% for all combination paths due to the coatings and combiner architecture.

ACKNOWLEDGMENTS AND FUNDING

SPECIAL THANKS TO NEW MEXICO TECH PHYSICS DEPARTMENT, DR. DANIEL LOPEZ, & SPIE.

The Magdalena Ridge Observatory (MRO) is funded by Agreement No. N00173-01-2-C902 with the Naval Research Laboratory (NRL). MRO Interferometer is hosted by the New Mexico Institute of Mining and Technology (NMT) at Socorro, NM, USA, in collaboration with the University of Cambridge (UK).

- [1] Coatings being applied by *Optical Surface Technologies* , (2801 Unit E Broadbent Parkway N.E., Albuquerque, NM 87107)
- [2] Infrasil 301 substrates manufactured by *IC Optical Systems*, (190-192 Ravenscroft Road Beckenham, Kent BR3 4TW, United Kingdom)
- [3] Optimization was performed using the *Essential Macleod Optical Thin Film Design and Analysis* software package.

VISIBILITY FACTORS

There are three effects that can in principle reduce fringe visibility:

1. unequal beam intensities.
2. polarization difference between s and p.
3. group delay effects.

PART I: INTENSITY MISMATCH FACTORS

Some paths are very symmetric, such as path C-B, correlating to minimal effects on visibilities. Path C-B's RR/LT output is perfectly symmetric and highly idealized.(**Figure 8, Figure 9 (a), Figure 10 (a)**).
Others paths are less symmetric (paths containing a compensator plate or 33.33% beamsplitter); these paths show a greater effect on visibilities. Overall the effect of intensity mismatch is the largest contributor to visibility losses.

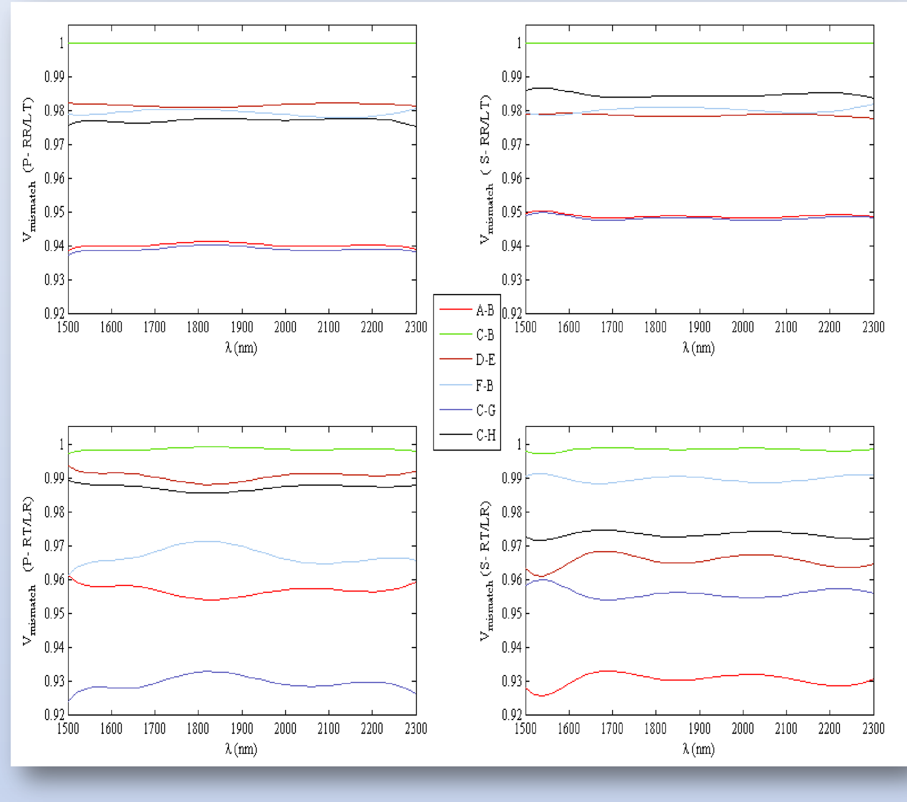

Fig 8 – (above right) Visibility factors as a function of wavelength due to intensity mismatch for the two combiner outputs (calculated using equation **(1)**).

PART II: POLARIZATION VISIBILITY FACTORS

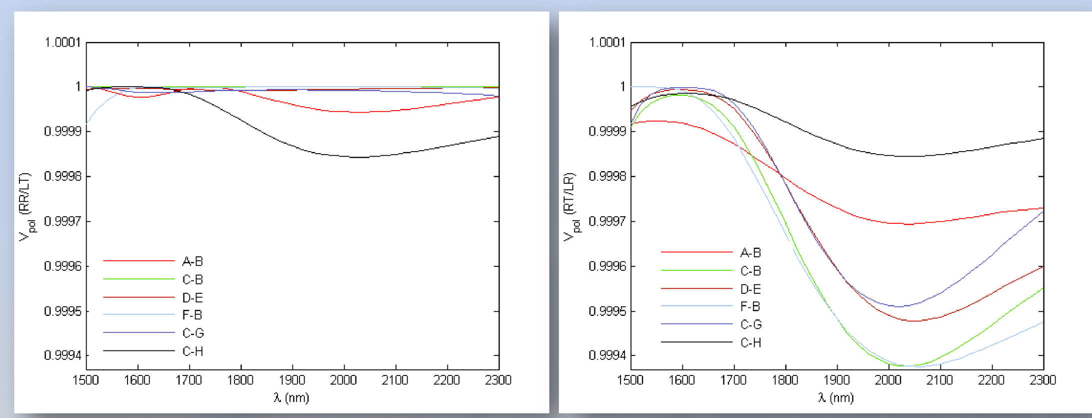

Visibility factors due to polarization were calculated using equation **(2)**. This loss in visibility is caused by the interference patterns of the s and p polarization states being slightly offset from each other; these effects are very small (<1.0%)(**Figure 9**).

Fig 9 (a)-(b) – Visibility factors due to polarization differences between s and p for combiner outputs (a) RR/LT and (b) RT/LR.

PART III: GROUP DELAY VISIBILITY FACTORS

Group delay is proportional to the rate of change of phase as a function of wave number evaluated at the center of the band (λ_H=1.65, λ_K=2.15); group delay factors were calculated from equation **(3)**. Effects from group delay are small (≤ 1.0%). (**Figure 10)**

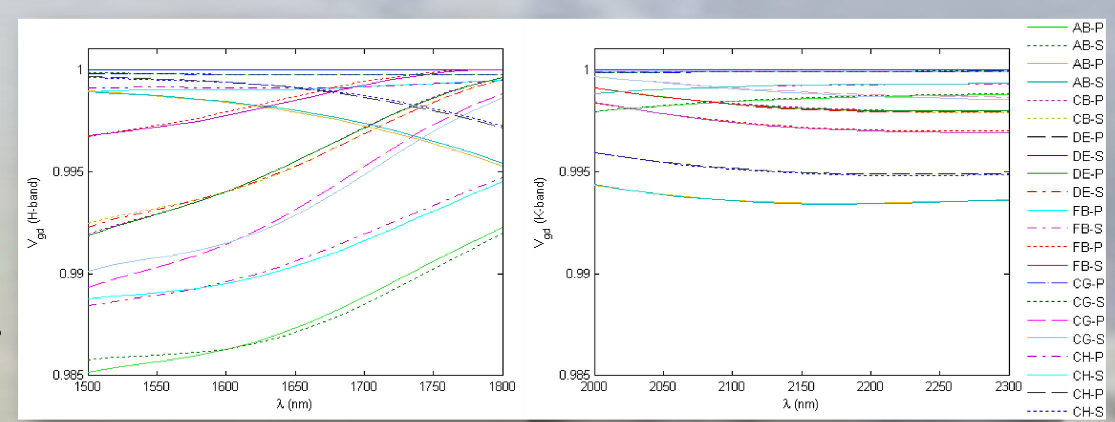

Fig 10 (a)-(b) – Trends in the visibility factors due to group delay for all paths, polarizations, and outputs for **(a)** H-band and **(b)** K-band. Parameters assumed for our modeling were: spectral resolution, R= 30, and coherence lengths of Λ_{coh} (H)=49.5 μm, and Λ_{coh} (K)= 64.5 μm.

PERFORMANCE: THEORETICAL VS. IDEAL

Figure 11 and **Tables 2- 5** provide a summary of calculated visibilities (V) in s and p polarization states normalized with the case of perfect coatings (V_{ideal}). Table comparisons were made at the mean wavelength in the H and K_s bands. Column "VI" in **Tables 2-5** show that the two emergent beams from outputs 1 and 2 (RR/LT & RT/LR) are roughly equal which is ideal. Performance of these coatings is excellent with visibility losses comparable (and in some cases slightly superior to) that of a combiner implementing perfect coatings. This is a result of the intensity mismatch being less with the coatings, than for the ideal case.

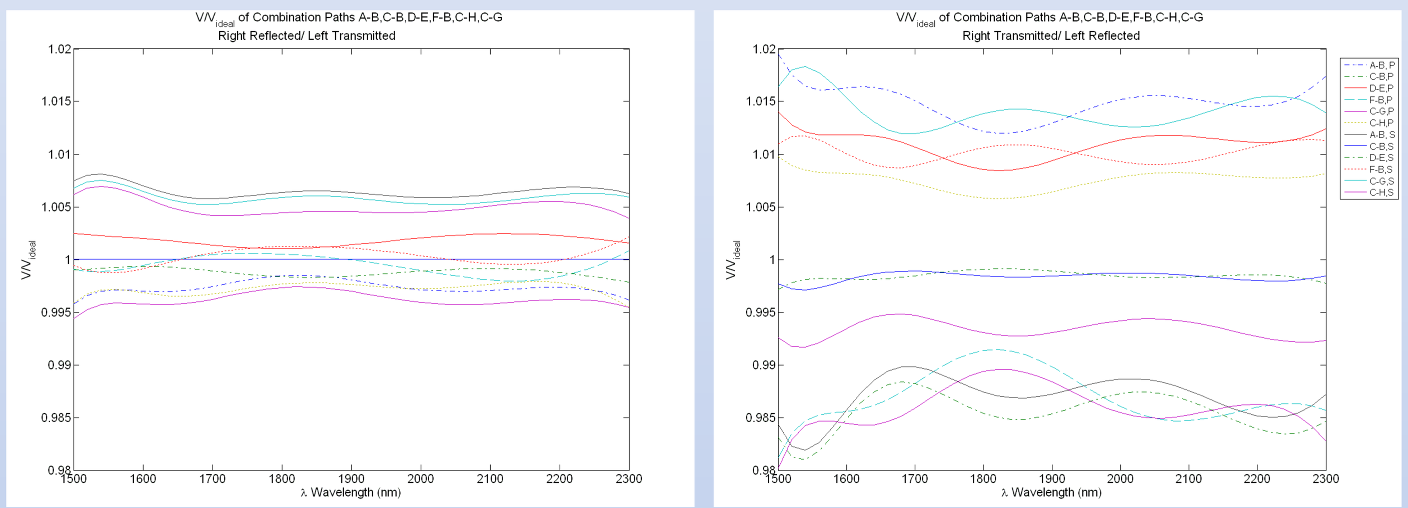

Fig 11 (a)-(b) – Calculated visibility ($V_{mismatch}$) normalized by the visibility assuming perfect coatings for (a) RR/LT and (b) RT/LR.

PATH	Wavelength (λ)		V	V_{ideal}	V/V_{ideal}	VI
A-B	Ks	1640	0.940	0.943	0.997	0.701
	H	2140	0.940	0.943	0.997	0.703
C-B	Ks	1640	1.000	1.000	1.000	0.492
	H	2140	1.000	1.000	1.000	0.493
D-E	Ks	1640	0.982	0.980	1.002	0.403
	H	2140	0.982	0.980	1.002	0.406
F-B	Ks	1640	0.980	0.980	1.000	0.401
	H	2140	0.978	0.980	0.998	0.398
C-G	Ks	1640	0.939	0.943	0.996	0.677
	H	2140	0.939	0.943	0.996	0.681
C-H	Ks	1640	0.976	0.980	0.997	0.395
	H	2140	0.978	0.980	0.998	0.398

Table 2

PATH	Wavelength (λ)		V	V_{ideal}	V/V_{ideal}	VI
A-B	Ks	1640	0.949	0.943	1.006	0.682
	H	2140	0.949	0.943	1.006	0.683
C-B	Ks	1640	1.000	1.000	1.000	0.491
	H	2140	1.000	1.000	1.000	0.493
D-E	Ks	1640	0.979	0.980	0.999	0.396
	H	2140	0.979	0.980	0.999	0.398
F-B	Ks	1640	0.980	0.980	1.000	0.401
	H	2140	0.979	0.980	1.000	0.401
C-G	Ks	1640	0.948	0.943	1.006	0.709
	H	2140	0.948	0.943	1.006	0.713
C-H	Ks	1640	0.985	0.980	1.005	0.412
	H	2140	0.985	0.980	1.005	0.414

Table 3

PATH	Wavelength (λ)		V	V_{ideal}	V/V_{ideal}	VI
A-B	Ks	1640	0.958	0.943	1.016	0.699
	H	2140	0.957	0.943	1.015	0.701
C-B	Ks	1640	0.998	1.000	0.998	0.490
	H	2140	0.998	1.000	0.998	0.492
D-E	Ks	1640	0.991	0.980	1.012	0.401
	H	2140	0.991	0.980	1.011	0.405
F-B	Ks	1640	0.966	0.980	0.986	0.400
	H	2140	0.965	0.980	0.985	0.398
C-G	Ks	1640	0.928	0.943	0.984	0.682
	H	2140	0.929	0.943	0.986	0.685
C-H	Ks	1640	0.988	0.980	1.008	0.394
	H	2140	0.988	0.980	1.008	0.397

Table 4

PATH	Wavelength (λ)		V	V_{ideal}	V/V_{ideal}	VI
A-B	Ks	1640	0.932	0.943	0.989	0.679
	H	2140	0.930	0.943	0.986	0.681
C-B	Ks	1640	0.999	1.000	0.999	0.489
	H	2140	0.998	1.000	0.998	0.491
D-E	Ks	1640	0.967	0.980	0.987	0.395
	H	2140	0.966	0.980	0.986	0.397
F-B	Ks	1640	0.989	0.980	1.009	0.399
	H	2140	0.989	0.980	1.010	0.400
C-G	Ks	1640	0.955	0.943	1.013	0.700
	H	2140	0.956	0.943	1.014	0.704
C-H	Ks	1640	0.974	0.980	0.995	0.410
	H	2140	0.973	0.980	0.994	0.413

Table 5

Tables 2-5 – These tables show the visibility (V), ideal visibility (V_{ideal}), visibility*intensity (VI), and visibility normalized by the ideal (V/V_{ideal}). **Table 2:** p-polarization and combiner output RR/LT. **Table 3:** s-polarization and combiner output RR/LT. **Table 4:** p-polarization and combiner output RT/LR. **Table 5 :** s-polarization and combiner output RT/LR..